Thin Solid Films 519 (2010) 1387–1390

Contents lists available at ScienceDirect

Thin Solid Films

journal homepage: www.elsevier.com/locate/tsf

Analytical modeling of wetting dependence on surface nanotopography

Zirong Tang [a], Rizwan Malik [b], Tielin Shi [b], Xiaotao Wang [b], Ping Peng [b], Xiaoping Li [a], Wuxing Lai [b], Shiyuan Liu [b,*]

[a] Wuhan National Laboratory for Optoelectronics, Huazhong University of Science and Technology, Wuhan 430074, China
[b] State Key Laboratory of Digital Manufacturing Equipment and Technology, Huazhong University of Science and Technology, Wuhan 430074, China

ARTICLE INFO

Article history:
Received 2 April 2010
Received in revised form 21 September 2010
Accepted 22 September 2010
Available online 1 October 2010

Keywords:
Wetting
Modeling
Hydrophilicity
Atomic force microscopy
Surface topography

ABSTRACT

An analytical model was developed to describe the mechanism of wetting dependence on surface nanotopography. This model relates the contact angle formation with the asperity geometry for application to a hydrophilic wafer surface, which is derived based on liquid–solid interfacial contact over the contact line. Experimental investigations were performed to verify the model. For much of the examined parameter room in the hydrophilic silicon wafer surface, it was found that the contact angle was strongly dependent on the ratio of asperity height to length, and the sharper asperity led to the higher contact angle. The observations are well consistent with Gibbs' contact-line theory.

1. Introduction

Wetting, as one of the most important properties of solid surfaces, has been widely used, from fundamental material research to many practical processes [1]. The wettability of a surface is commonly characterized by the static contact angle between a liquid droplet and the surface, which is mainly governed by solid–liquid interface chemistries and surface micro-nano geometries [2,3]. Apart from the chemical nature, the contact angle of a liquid drop dispensed onto a solid surface is not unique but can vary over a finite range. The topography of the surface influences this range of contact angles. In the past few years, many experimental results have confirmed that wettability can be tuned by surface geometry. Roughening the surface can enhance its repellent or wetting properties, resulting in "superhydrophobic" or "superhydrophilic" textures [4]. Wenzel [5] and Cassie [6] have initially published a relationship between physical structure and contact angle through the liquid–solid interfacial area. In the literature, quantitative agreements between experimental contact angles and those predicted by the Wenzel and Cassie equations have sometimes been claimed [7–12], yet many examples where they are inconsistent have also been reported [1,13]. It is obvious that Wenzel and Cassie equations do not fully account for the geometry of the surface such as the feature shape. Furthermore, when the surface roughness is not in a regular pattern, it is hard to incorporate the geometry factors into consideration. It is also argued that contact angles are not determined by the liquid–solid interfacial area since wetting is controlled by interactions at the contact line [14–18]. Generally, for the systems with a high degree of roughness or nanotopography, the picture of wetting and its roughness dependence are not conclusive. On the other hand, many researchers have contributed to the fabrication and understanding of superhydrophobic surfaces, and most of the theories for both hydrophobic and hydrophilic rough surfaces have been tested by preparing surfaces structured on the micrometer scale. Only few studies have been done recently on the surface with nanotopograhies [18–23], mainly because of the difficulty of fabrication, and much less work has been dedicated to the study of superhydrophilic surfaces [19,21,22].

With the development of silicon-based technology, the surface topography of the silicon substrate can be tuned to be within nanoscale range and its superhydrophilicity can also be achieved through drying (plasma and photoinduced approach) or wet chemical treatment. With the advent of atomic force microscopy (AFM), the characteristics of surface nanotopography can be obtained [24]. However, when the surface topographies are in nano-scale range, the structure patterns are usually in random distribution, which are commonly described by a statistical approach. As yet no analytical approaches are available to determine the role of surface nanotopography on wetting. In this research, we will propose an analytical model based on the liquid–solid contact-line theory with special attention to wetting dependence on the nanotopographic surface. The geometry of the surface will be fully considered, and experimental investigations with the hydrophilic silicon substrate will be conducted to examine the model.

* Corresponding author.
E-mail address: shyliu@mail.hust.edu.cn (S. Liu).

0040-6090/$ – see front matter © 2010 Elsevier B.V. All rights reserved.
doi:10.1016/j.tsf.2010.09.047

2. Theoretical model

Gibbs has proposed a simple geometric relation that describes the interaction of liquids with solid sharp edges a long time ago, which demonstrated the contact angle formation with the advance of the contact line between the liquid and the rectilinear edge of solid [2]. In many cases, the real facets of the solid surface can be curved. Extrand has improved Gibbs' model for the case of the spherical surface recently [16]. In the present work, an analytical model will be developed for the surface with nanotopography following the contact-line theory. Taking wavelength of asperity as a measure, the surface roughness distribution can be described by the sinusoidal function [25]. Assuming that the surface nano-scale profile is periodically rough as shown in Fig. 1(a), the surface roughness is illustrated by a two-dimensional schematic drawing of asperities, which can be given by the following equation.

$$f(x) = h\cos^2\left(\frac{\pi x}{L}\right) \tag{1}$$

where $x \in (-kL/2, kL/2)$, k is an integer, L and h are the length and height of asperity, respectively.

When a liquid microdrop is deposited on the surface as presented in Fig. 1(b), and assuming that the drop is symmetrical with the axis y, then the static contact angle θ_a can be described by the following equation.

$$\theta_a = \theta_{a,o} + \theta \tag{2}$$

where $\theta_{a,o}$ is the original contact angle when no roughness is introduced, and θ is the advanced contact angle due to the effect of roughness, which is the tangential angle of the asperity curve at the any point x. Therefore, θ can be calculated from the derivation of the following equation.

$$\tan\theta = f'(x) \tag{3}$$

From Eq. (1), we get

$$f'(x) = -\frac{\pi h}{L}\sin\frac{2\pi x}{L} \tag{4}$$

then

$$\tan\theta = \frac{\pi h}{L}\sin\frac{2\pi x}{L}, x \in \left(0, \frac{L}{2}\right). \tag{5}$$

Let $\gamma = \frac{S_x}{S_L} = \frac{4\pi x^2}{\pi L^2}$, where S_x is the lateral circular area of the asperity at the position x, and S_L is the circular area at asperity bottom position $x = L/2$, then, $\frac{x}{L} = \frac{\sqrt{\gamma}}{2}$, and we get

$$\theta = \arctan\left(\frac{\pi h}{L}\sin\pi\sqrt{\gamma}\right). \tag{6}$$

Then Eq. (2) becomes

$$\theta_a = \theta_{a,o} + \arctan\left(\frac{\pi h}{L}\sin\pi\sqrt{\gamma}\right). \tag{7}$$

The above equation predicts the contact angle for sinusoidal distributed surface topography, where γ is the ratio of the lateral circular area of asperity at any position x to that of the bottom position $x = L/2$, which illustrates the degree of sharpness at the line edge of asperity. For the case when the surface is initially completely wetted, $\theta_{a,o}$ is equal to 0 and x is at the location of $L/4$, and γ is equal to 1/4, Eq. (7) becomes

$$\theta = \arctan\left(\frac{h}{L}\pi\right). \tag{8}$$

Eq. (8) shows that the contact angle is dependent on h and L, where h is calculated through another key parameter root-mean-square (RMS), that is $h = 2\mathrm{RMS}$. Both RMS and L can also be obtained through surface characterizations.

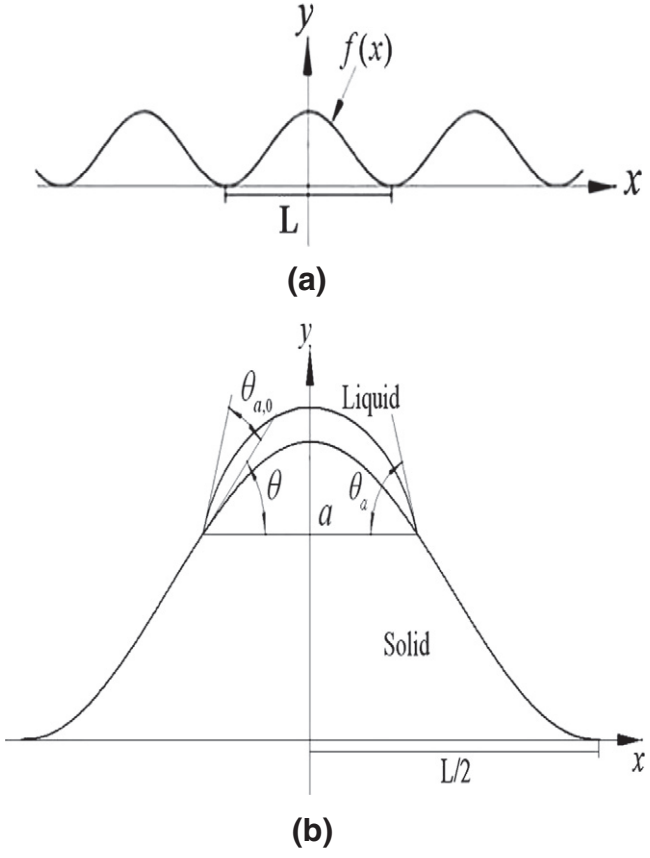

Fig. 1. (a) Surface nanotopography modelled by the sinusoidal function. (b) Relation of the contact angle formation with the surface asperity geometry.

3. Experimental details

To verify the above model, we use a silicon wafer as an experimental model system, since its surface can be modified and wettability can be tuned to be hydrophilic or superhydrophilic through mature surface treatment procedures [26]. In our experiment, single-side polished p-type (111) standard wafers with a thickness of 380 μm and RMS of around 6 nm were selected. After chemical mechanical polishing, the wafers were diced into small pieces as original samples for hydrophilicity enhancement and wetting experiments. Samples were modified through the following wet chemical treatments to achieve strong hydrophilic surfaces. (1) Samples were cleaned by acetone in supersonic cleaner for 20 min to remove most of the organic contaminations. (2) Samples were boiled in a mixture of hydrogen peroxide and sulfuric acid (volume ratio H_2SO_4:H_2O_2 = 2:1) for 20 min to eliminate metal particle contaminations. (3) Samples were dipped in dilute hydrofluoric acid for 30 s to remove the native oxide layer from surfaces. (4) Samples were immersed in a modified RCA1 solution (volume ratio NH_4OH: H_2O_2: H_2O = 1:1:5) for duration of 5 min to 30 min at a temperature of 25 °C or 50 °C. Deionized water flushing was followed after each step. Finally the substrates were spin-dried after rinsing. By varying the immersion durations and temperatures of substrates in the RCA1 solution, the surface roughness with different groups of surface characteristics was accomplished, and the

Table 1
Sample surface modifications, characterizations and contact angle measurements[+].

Group no#	Surface treatments	L (μm)	RMS (nm)	h/L (10^{-3})	Static CA (°)
1	50 °C, RCA1, 30 min	0.121–0.273	1.5	11–24.77	5.21 ± 0.25
2	50 °C, RCA1, 25 min	0.11–0.25	1.5	12.01–27.18	5.60 ± 0.35
3	50 °C, RCA1, 15 min	0.081–0.182	1.5	16.51–37.22	8.25 ± 0.35
4	50 °C, RCA1, 5 min	0.12–0.276	2.5	18.13–40.83	9.11 ± 0.45
5	25 °C, RCA1, 30 min	0.11–0.227	2.5	21.98–45.3	8.35 ± 0.45
6	25 °C, RCA1, 25 min	0.109–0.204	2.5	24.49–45.7	9.25 ± 0.45
7	25 °C, RCA1, 15 min	0.161–0.309	5	32.39–62.21	10.42 ± 0.5
8	25 °C, RCA1, 5 min	0.125–0.267	5	37.39–80.01	13.41 ± 0.5

[+]All data are measured and calculated from one cross-section profile with a AFM scan area of $10 \times 10\ \mu m^2$, h = 2RMS, CA = contact angle.

surface became hydrophilic after modification. As presented in Table 1, 8 groups of substrate having 10 samples in each group were modified with the above hydrophilic enhancement process. Nanotopographies of these samples were characterized by AFM (Veeco Instruments Inc., Nanoscope Multi-mode) with contact-mode and SiN probe of triangular shape, and further measurements of contact angles for wettability were conducted for samples of each group.

When pure water was applied to measure the contact angle, it was found that all hydrophically treated samples were completely wetted, which means that the hydrophilic treatment process was successful, and the initial contact angle $\theta_{a,o}$ could be regarded as zero. Then lower surface tension salted water (NaCl solution) with 30% volume concentration was applied to investigate the effect of surface nanotopography on wetting by measuring contact angles on the modified sample surfaces. Commercial contact angle measuring instrument (Automatic Contact Angle Meter Model SL200B from Sdon Information Technology Co., China) was applied in this experiment. The liquid droplet was dropped to the sample surface from a distance of 5 cm by vibrating the syringe. The volume of the liquid drop was controlled to be 2 μL each time. The sample plate was vibrating slightly before each measurement to obtain the static contact angle.

3. Results and discussions

Surface characteristics of each modified samples are determined through AFM image analysis. Fig. 2 shows AFM images for four typical surfaces, where Fig. 2(a), (b), (c) and (d) were obtained from different modification processes, respectively. The changes of surface roughness quality can be clearly observed with different RCA1 immersion temperature and duration. Through AFM characterization [25], the asperity geometries (RMS and L) were obtained for samples of each group and details were presented in Table 1. Fig. 3 is the section analysis of a typical surface AFM image, where the RMS value is around 1.5. From the analysis, it is observed that the surface nanoscale roughness distribution displays closely a periodical profile of asperities, which supports the previous assumption for surface roughness modeling. It was illustrated that although RMS was almost constant for each group, whilst the asperity length was in a wide range, which means that surface nanotopographies must be closely modeled as a mix of wide range sinusoidal groups.

Taking asperity data (RMS and L) from the AFM image of the treated sample surface, the corresponding contact angle can be calculated from Eq. (8), where h is equal to 2RMS in the model. It is worth saying that Wenzel or Cassie models always predict that the surface

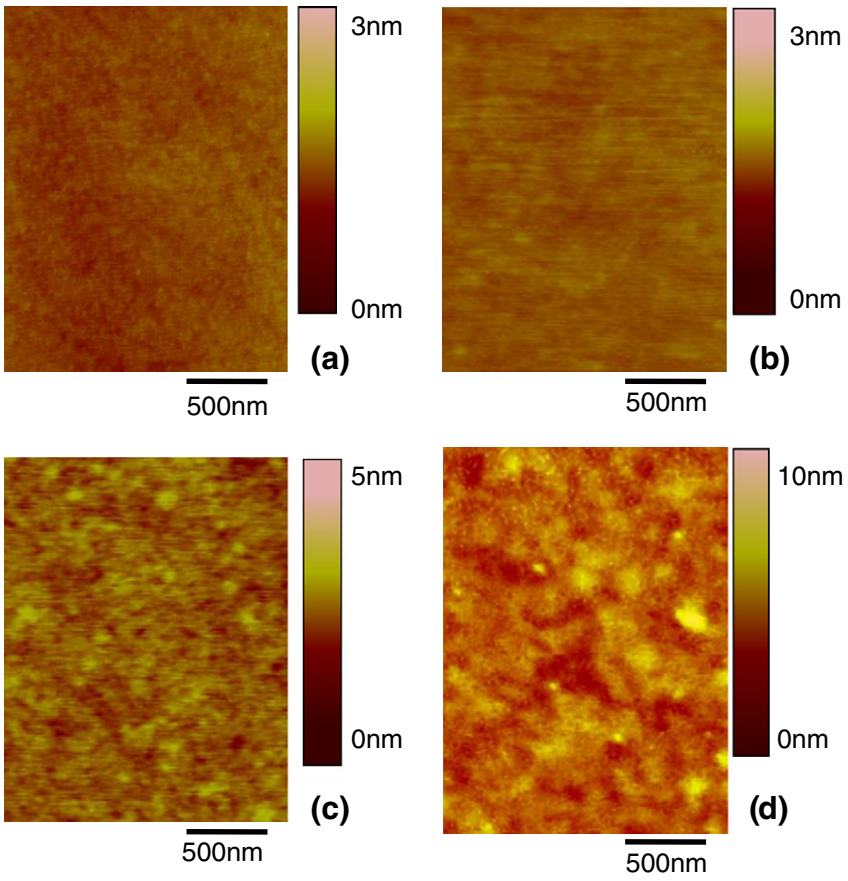

Fig. 2. AFM images of sample surfaces after chemical treatments. (a) 50 °C, RCA1 immersion, 30 min, (b) 50 °C, RCA1 immersion, 5 min, (c) 25 °C, RCA1 immersion, 30 min, and (d) 25 °C, RCA1 immersion, 5 min.

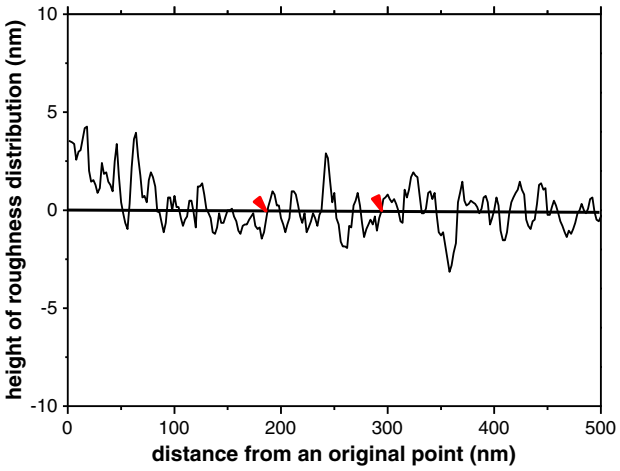

Fig. 3. Section analysis of a typical AFM image with RMS of around 1.5.

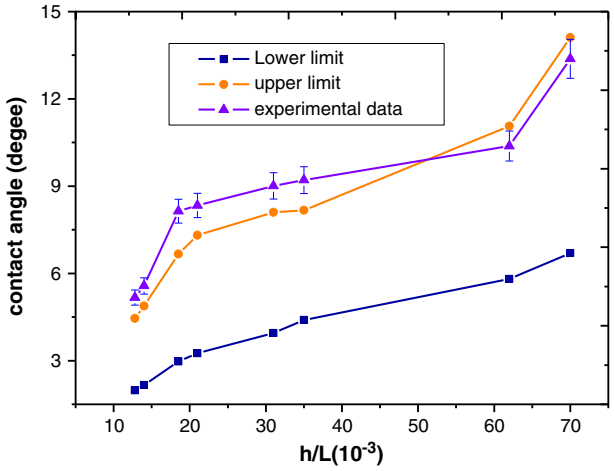

Fig. 5. Comparison of contact angles between theoretical calculations and experimental measurements.

roughness will make the hydrophobic surface to be more hydrophobic and the hydrophilic surface to be more hydrophilic, therefore they are not applicable for the case when the sample surface is completely wetted initially (i. e. $\theta_{a,o}$ is equal to 0).

From contact angle measurements, the results of 10 samples from each group were obtained and presented in Table 1. Fig. 4 shows 8 typical static contact angle images measured as 5.17°, 5.57°, 8.14°, 8.34°, 9.01°, 9.21°, 10.38°, and 13.38° from each sample group of 1 to 8 respectively, and the measurement error was from 0 to 1°. Then theoretical predictions and experimental measurements can be compared. Fig. 5 plots the contact angle from both theoretical calculations and experimental measurements, where the upper limit data were calculated from the highest h/L values of each group, while the lower limit data are from the lowest h/L values of each group. In Fig. 5, it is also shown that the surface nanotopography affects the formation of the static contact angle. Since the liquid microdrop was deposited on the surface covering more than one asperity, the change of the static contact angle must be due to the overall effects of all asperities being seated, which is statistically described by the ratio range of h/L as shown in Table 1. Furthermore, it is also found that the contact angles of experimental measurements were very close to the upper limit data of the theoretical predictions, which means that the sharper asperities of the surface nanotopogrphies play a dominant role in determining the contact angle.

The observations here proved that the dominant factor for contact angle formation was the liquid–solid contact line, which is consistent with Gibbs' and Extrand's conclusions [2,16]. This analysis also agrees with McHale's argument that some solid has a roughness induced hydrophobic tendency [10].

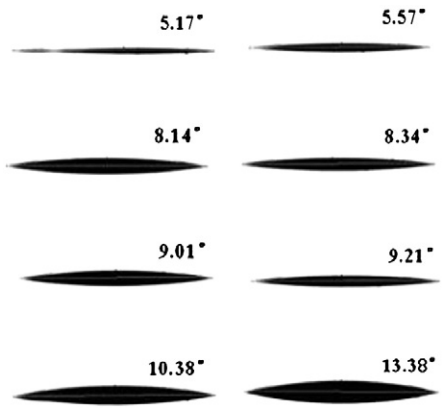

Fig. 4. Typical contact angle images obtained from each sample group.

4. Conclusions

In summary, we have developed a quantitative description of the contact angle dependence on the sinusoidal distributed nano-scale surface. The proposed contact-line model was validated for relating the contact angle formation with nanotopographies for the hydrophilic surface. It is concluded that sharper asperities dominate the contact angle formation, and the shaper asperity leads to the higher contact angle. The observations in this work provide an insight view for the wetting dependence on the surface roughness at nano-scale.

Acknowledgements

The work is financially supported by National Natural Science Foundation of China (nos. 90923019, 50875103, 50775090, and 50975114) and Wuhan National Laboratory for Optoelectronics.

References

[1] T.T. Chau, W.J. Bruckard, P.T.L. Koh, A.V. Nguyen, Adv. Colloid Interface Sci. 150 (2009) 106.
[2] J.W. Gibbs, the Collected Works of J. Willard Gibbs, Yale University Press, New Haven, CT, 1961.
[3] S. Veeramasuneni, J. Drelich, J.D. Miller, G. Yamauchi, Prog. Org. Coat. 31 (1997) 265.
[4] J. Bico, C. Tordeux, D. Quere, Europhys. Lett. 55 (2001) 214.
[5] R.N. Wenzel, Ind. Eng. Chem. 28 (1936) 988.
[6] A.B.D. Cassie, S. Baxter, Trans. Faraday Soc. 40 (1944) 546.
[7] N.A. Patankar, Lamgmuir 20 (2004) 7097.
[8] C. Dorrer, J. Ruhe, Langmuir 24 (2008) 1959.
[9] E. Bormashenko, R. Pogreo, G. Whyman, Y. Bormashenko, M. Erlich, Appl. Phys. Lett. 90 (2007) 201917.
[10] G. McHale, Langmuir 25 (2009) 7185.
[11] B. Bhushan, Y.C. Jung, J. Phys.:Condens. Matter. 20 (2008) 225010.
[12] K. Tsougeni, N. Vourdas, A. Tserepi, E. Gogolides, C. Cardinaud, Langmuir 25 (2009) 11748.
[13] Y.V. Kalinin, V. Berejnov, R.E. Thorne, Langmuir 25 (2009) 5391.
[14] C.W. Extrand, Langmuir 19 (2003) 3793.
[15] C.W. Extrand, S.I. Moon, D. Schmidt, Langmuir 23 (2007) 8882.
[16] C.W. Extrand, S.I. Moon, Langmuir 24 (2008) 9470.
[17] L. Gao, T.J. Marcarthy, Langmuir 23 (2007) 3762.
[18] T. Ondarcuhu, A. Piednoir, Nano Lett. 5 (2005) 1744.
[19] E. Martines, K. Seunarine, H. Morgan, N. Gadegaard, C.D.W. Wilkinson, M.O. Riehle, Nano Lett. 5 (2005) 2097.
[20] Z. Wang, N. Koratkar, L. Ci, O.M. Ajayan, Appl. Phys. Lett. 90 (2007) 143117.
[21] D.X. Ye, T.M. Lu, Phys. Rev. Lett. 100 (2008) 256102.
[22] C. Yang, U. Tartaglino, B.N.J. Persson, The Eur. Phys. J. E. 25 (2008) 139.
[23] G. Londe, A. Chunder, L. Zhai, H.J. Cho, Appl. Phys. Lett. 94 (2009) 164104.
[24] C. Cui, M. Elwenspoek, N. Tas, J.G.E. Gardeniers, J. Appl. Phys. 85 (1999) 7448.
[25] Z. Tang, T. Shi, G. Liao, S. Liu, Microelectron. Eng. 85 (2008) 1754.
[26] Q. Tong, U. Gosele, Semiconductor Wafer Bonding: Science and Technology, Wiley, New York, 1999.